# Path-Parameterization Approach Using Trajectory Primitives for Three-Dimensional Motion Planning

Abraham J. Pachikara[1]; Joseph J. Kehoe[2]; and Rick Lind[3]

**Abstract:** Motion planning determines trajectories for vehicles that link an initial location and heading with a final location and heading. Techniques for motion planning have been developed for two-dimensional maneuvering; however, they are less mature for three-dimensional maneuvering. The concept of motion primitives is particularly attractive for motion planning that determines trajectories as a set of maneuvers that satisfy differential constraints. This paper furthers work on a higher-level abstraction of trajectory primitives that consider sequences of motion primitives. In this paper, trajectory primitives are developed that deal with airspace constraints of an environment. The motion planning is shown to be an optimization involving a pair of trajectory primitives that is related by an intermediate waypoint. The resulting path is completely parameterized by the waypoint location. **DOI: 10.1061/(ASCE)AS.1943-5525.0000152.** 

**CE Database subject headings:** Aircraft; Optimization; Simulation; Planning.

**Author keywords:** Aircraft; Optimization; Simulation; Guidance; Motion planning.



## Introduction

Autonomous operation of aircraft requires some capability to determine trajectories along which the vehicle should fly. Techniques for such determination are relatively mature for vehicles that fly at high altitude in open airspace using nearly two-dimensional (2D) maneuvering; however, techniques are not nearly as mature for small aircraft that require fully three-dimensional (3D) maneuvering while immersed in an urban environment. Also, the computation time for such planning must be extremely low to allow for rapid path generation as new environmental features are identified.

Extending 2D techniques to a 3D environment is not necessarily trivial. The motion of aircraft, with associated differential and dynamical constraints, adds considerable complexity to the motion planning. Such an extension used mixed-integer linear programming to compute trajectories by constructing a map of feasible paths and then selecting the optimal one; however, the computational time was considerable even with a simple model of the dynamics (Kuwata and How 2004).

The concept of basic maneuvers, or motion primitives, enables a type of motion planning by considering a complicated trajectory as being composed of several simple maneuvers. A critical foundation was established by Dubins (1957) for a 2D car (Shkel and Lumelsky 2001). The concept of a Dubins car provides a closed-form solution for optimal trajectories and has been used for many types of planning, such as the traveling-salesman problem (Le Ny and Feron 2005). This foundation is used for several studies into aircraft motion, but the process limits that motion to a 2D plane (Howlett et al. 2003; McGee and Hedrick 2007; Tang and Ozguner 2005; Yang and Kapila 2002; Shima et al. 2007; Grymin and Crassidis 2009; Sujit and Beard 2007; Zollars et al. 2007; Scholer et al. 2009; Larson et al. 2005; Shanmugavel et al. 2005). One approach expands the original 2D formulation into a 3D framework, but it does not deal with constraints in the climb rate or specific values of these climb rates corresponding to trim conditions, as is the case with motion primitives (Shanmugavel et al. 2006). Another variation noted the lack of algebraic solutions for 3D planning using a Dubins airplane, and therefore considered genetic algorithms (Malaek and Nabavi 2010). Complete analogs to the Dubins car in 3D are still being developed to account for the shortest path between two points with associated heading constraints (Chitsaz and LaValle 2007) and heading and flight-path angle constraints (Ambrosino et al. 2006). Furthermore, existing approaches often require all primitives to have a uniform velocity and turn radius along with a climb rate, even though such uniformity is not realistic for most aircraft.

The paper introduces an efficient approach to parametrize paths for fully 3D motion planning. The approach depends on the concept of trajectory primitives as higher-level abstractions representing sequential transformations of motion primitives. Motion primitives represent typical or useful motions for flight; similarly, trajectory primitives represent typical or useful trajectories for flight. The motion planning is shown to be simply a search over a low-dimensional subspace, being only $\mathcal{R}^1$, $\mathcal{R}^2$, or $\mathcal{R}^3$, depending on the type of primitive, to find a waypoint that relates a pair of trajectory primitives. Each of these separate trajectory primitives is computed from a closed-form algebraic solution, which is easily computed. As such, the complicated problem of motion planning is reduced to a low-dimensional optimization using these trajectory primitives as parametrized over a waypoint.

This inclusion of the waypoint is critical for situations in which the time to climb to the desired altitude is greater than the time to travel to the desired North-East location. The simplest situation would have the vehicle climb or dive at maximum rate until reaching the desired altitude and then continue using a 2D solution until reaching the final configuration (Hurley et al. 2009); however, that

[1]Graduate Student, Dept. of Mechanical and Aerospace Engineering, Univ. of Florida, Gainesville, FL 32611. E-mail: ajpach@ufl.edu

[2]Senior Systems Engineer, Scientific Systems Co., Inc., 500 W. Cummings Park, Woburn, MA 01801. E-mail: joseph.kehoe@ssci.com

[3]Associate Professor, Dept. of Mechanical and Aerospace Engineering, Univ. of Florida, Gainesville, FL 32611 (corresponding author). E-mail: ricklind@ufl.edu

Note. This manuscript was submitted on September 17, 2010; approved on July 20, 2011; published online on July 22, 2011. Discussion period open until December 1, 2013; separate discussions must be submitted for individual papers. This paper is part of the ***Journal of Aerospace Engineering***, Vol. 26, No. 3, July 1, 2013. ©ASCE, ISSN 0893-1321/2013/3-571–585/$25.00.

approach is infeasible when the rate of change of altitude is too small. The inability to move vertically for many aircraft requires the trajectory to add horizontal distance and provide sufficient time for the vehicle to change altitude.

Also, the approach is formulated to account for variations in velocities and rates between various maneuvers. The concept of similarity is used to generate identical trajectories from primitives that have different parameters. The planning generates a pair of trajectory primitives using 2D Dubins solutions but has the aircraft follow trajectory primitives in 3D space, whose 2D projections have this similarity property to the optimal 2D primitives. In this way, the optimality of the 2D results is not maintained; however, the allowance for varying velocities and rates between maneuvers is added.

## Trajectory Primitives

### Motion Primitives

A family of motion primitives is generated using a Dubins airplane. This concept arises by extending the family of 2D trajectories associated with the classic Dubins car (1957) into 3D trajectories (Shanmugavel et al. 2006; Chitsaz and LaValle 2007). The basic concept considers motion that can be straight or turning with altitude that can remain constant or change as a result of diving or climbing.

The kinematic model operates in a configuration space of $\mathcal{C}^4$ spanned by three Euclidean position variables, $(p_x, p_y, p_z) \in \mathcal{R}^3$, and an angle of $\psi \in \mathcal{R}$, which describes heading. The vehicle is constrained during motion to having a constant velocity of $V > 0 \in \mathcal{R}$, a constant turn rate of $\omega \in \mathcal{R}$, and a constant rate of change of altitude given as $\gamma \in \mathcal{R}$. The resulting states are governed by Eq. (1)

$$\begin{bmatrix} \dot{p}_x \\ \dot{p}_y \\ \dot{p}_z \\ \dot{\psi} \end{bmatrix} = \begin{bmatrix} V\cos\psi \\ V\sin\psi \\ \gamma \\ \omega \end{bmatrix} \tag{1}$$

The trajectories associated with the model in Eq. (1) represent maneuvers that the vehicle can perform. Most aircraft have a range of velocities and rates over which they can trim; consequently, it is reasonable to define a set of parameters such that $\Omega = (\omega_1, \ldots, \omega_n)$ represents the set of possible turn rates and $\Gamma = (\gamma_1, \ldots, \gamma_m)$ represents the set of possible climb rates. The velocity can also vary within the set of $\mathcal{V} = (V_1, \ldots, V_p)$.

A set of motion primitives is then defined that represents all possible maneuvers. Each element in this set is a trajectory defined by the time-varying values of position and orientation during the maneuver. As such, any motion primitive, $X \in \mathcal{X}$, is parametrized by a velocity of $V$ and a duration of the maneuver, $\tau > 0$, along with turn rate, $\omega$, and climb rate, $\gamma$, as given in Eq. (2)

$$\mathcal{X} = \left\{ X(\tau, V, \omega, \gamma) : X = \int_0^{\tau} \begin{bmatrix} V\cos\psi \\ V\sin\psi \\ \gamma \\ \omega \end{bmatrix} dt, V \in \mathcal{V}, \omega \in \Omega, \gamma \in \Gamma \right\} \tag{2}$$

A critical feature of this set is the notion of feasibility. Essentially, any member, $X \in \mathcal{X}$, is constrained, and therefore the evolution of the trajectory is constrained by the differential relationship in Eq. (1). The resulting set is a collection, or library, of feasible maneuvers that can be achieved by the vehicle.

A motion primitive, $X(\tau_2 - \tau_1, V, \omega, \gamma) \in \mathcal{X}$, represents a trajectory of the vehicle with a turn rate of $\omega \in \Omega$ and a climb rate of $\gamma \in \Gamma$, which lasts for a duration of $\tau_2 - \tau_1$. A vehicle starting at an initial configuration of $C_o \in \mathcal{C}^4$ at time $\tau_1$ that undergoes this motion primitive will reach a final configuration of $C_f \in \mathcal{C}^4$ at time $\tau_2$, as shown in Eq. (3)

$$C_o + X(\tau_2 - \tau_1, V, \omega, \gamma) = C_f \tag{3}$$

Velocity is described as the inertial rate of change of position. In practice, such a velocity may be a combination of vehicle airspeed and wind, which could affect the primitive and associated motion.

### Trajectory Primitives

The concept of motion primitives as canonical motion segments is extended to canonical trajectory segments using trajectory primitives. Trajectory primitives are generated by concatenating a group of motion primitives such that one starts at a time and location corresponding to the finish of another. The amount of time, and associated range of motion, can vary between primitives within the same sequence. Thus, these sequences can represent complex maneuvers for which the motion primitives form a basis.

A set of trajectory primitives associated with a one-primitive sequence is defined in Eq. (4). This primitive is obviously the trivial case of turning; however, it is defined for convenience in notation. The traditional use of Dubins' paths would never have any turn lasting a complete revolution, whereas the paths using $\mathcal{T}_1$ will often require many revolutions. The primitive of $T \in \mathcal{T}_1$ with $T = X_1$ is intended to note that if $C_o + X_1 = C_f$ then $C_o + T = C_f$ for some configurations of $C_o \in \mathcal{C}^4$ and $C_f \in \mathcal{C}^4$

$$\begin{aligned} \mathcal{T}_1 = [&T(t_1, V_1, \omega_1, \gamma_1) : T(t_1, V_1, \omega_1, \gamma_1) \\ &= X_1(t_1, V_1, \omega_1, \gamma_1), \quad X_1 \in \mathcal{X}] \end{aligned} \tag{4}$$

A set of trajectory primitives associated with two-primitive sequences is defined in Eq. (5) as $\mathcal{T}_2$. These sequences are restricted to a turn primitive followed by a straight primitive. The turn can be either positive or negative; however, the order of the turn followed by the straight will be enforced for this set. Also, the time of each primitive is noted as $t_1$ or $t_2$ to reflect that the length of each maneuver may vary within the sequence. The trajectory primitive of $T \in \mathcal{T}_2$ with $T = X_1 + X_2$ is intended to note that if $C_o + X_1 + X_2 = C_f$ then $C_o + T = C_f$ for some configurations of $C_o \in \mathcal{C}^4$ and $C_f \in \mathcal{C}^4$

$$\begin{aligned} \mathcal{T}_2 = [&T(t_1, t_2, V_1, V_2, \omega_1, 0, \gamma_1, \gamma_2) : T(t_1, t_2, V_1, V_2, \omega_1, 0, \gamma_1, \gamma_2) \\ &= X_1(t_1, V_1, \omega_1, \gamma_1) + X_2(t_2, V_2, 0, \gamma_2), \quad X_1, X_2 \in \mathcal{X}] \end{aligned} \tag{5}$$

A set of three-primitive sequences is also defined. This set of trajectory primitives, given as $\mathcal{T}_3$ in Eq. (6), consists of various combinations of turn primitives and straight primitives. The order may vary between sequences, but each is restricted to a combination of three primitives

$$\begin{aligned} \mathcal{T}_3 = [&T(t_1, t_2, t_3, V_1, V_2, V_3, \omega_1, \omega_2, \omega_3, \gamma_1, \gamma_2, \gamma_3) : \\ &T(t_1, t_2, t_3, V_1, V_2, V_3, \omega_1, \omega_2, \omega_3, \gamma_1, \gamma_2, \gamma_3) \\ &= X_1(t_1, V_1, \omega_1, \gamma_1) + X_2(t_2, V_2, \omega_2, \gamma_2) \\ &+ X_3(t_3, V_3, \omega_3, \gamma_3), \quad X_1, X_2, X_3 \in \mathcal{X}] \end{aligned} \tag{6}$$



J. Aerosp. Eng. 2013.26:571-585.

Finally, a set of trajectory primitives associated with four-primitive sequences is defined in Eq. (7) as $\mathcal{T}_4$. The motion allows for revolutions by repeating a pattern of turns and straights with the turns being either both positive or both negative. The primitive begins with a partial turn or straight, followed by the repeating pattern, and then ends with a partial completion of the pattern. The initial primitive has a duration of $t_1$, whereas the duration of the straight motion within the repeating pattern has a duration of $t_2$; the total duration of the entire motion is $t_T$. The time of each turn within the repeating turn is defined as $t_t$, which relates the duration required to turn a half circle. The number of repetitions, $N$, is generated by the durations to satisfy $t_1 + N2(t_2 + t_t) + t_4 = t_T$, because the initial time plus the repetition time and the final time must equal the total time. In this way, the four-primitive sequence generates a Cassini oval

$$\begin{aligned}\mathcal{T}_4 = \Big[&T(t_1,t_2,t_T,V_1,V_2,\omega_1,\omega_2,\gamma_1,\gamma_2):\\ &T(t_1,t_2,V_1,V_2,\omega_1,\omega_2,\gamma_1,\gamma_2) = X_1(t_1,V_1,\omega_1,\gamma_1)\\ &+\sum_{i=1}^{N}[X_2(t_2,V_2,\omega_2,\gamma_2) + X_1(t_t,V_1,\omega_1,\gamma_1)\\ &+X_2(t_2,V_2,\omega_2,\gamma_2) + X_1(t_t,V_1,\omega_1,\gamma_1)]\\ &+(X_2\{\min[t_T - t_1 - N2(t_2+t_t),t_2],V_2,\omega_2,\gamma_2\}\\ &+X_1\{\min[t_T - t_1 - N2(t_2+t_t) - t_2,t_1],V_1,\omega_1,\gamma_1\}\\ &+X_2\{\min[t_T - t_1 - N2(t_2+t_t) - t_2 - t_1,t_2],V_2,\omega_2,\gamma_2\}\\ &+X_1\{\min[t_T - t_1 - N2(t_2+t_t) - t_2 - t_1 - t_2,t_1],\\ &V_1,\omega_1,\gamma_1\}),\quad X_1,X_2 \in \mathcal{X}\Big]\end{aligned} \tag{7}$$

Fig. 1 shows examples of the aforementioned trajectory primitives. As will be subsequently shown, the first and third trajectory primitives will be useful for trajectories that may need to satisfy airspace constraints.

### Similarity

A motion primitive represents a trajectory, as determined by spatial locations and attitude orientations, along with the temporal value at which each location and orientation is reached. The differential constraints for the duration of time relate the motion primitive to such a trajectory. The turn rate and climb rate along with the velocity are constant during a trajectory, and therefore any primitive, $X \in \mathcal{X}$, maps time into the configuration space as $X: \mathcal{R} \to \mathcal{C}^4$.

A trajectory is not unique to a specific motion primitive when considering a scaling of velocity. Essentially, multiple motion primitives may reach the same spatial locations with the same attitude orientations but at different times because of differences in velocities. As such, two primitives of $X_1 \in \mathcal{X}$ and $X_2 \in \mathcal{X}$ are defined as being similar, $X_1 \sim X_2$, if they represent the same locations and orientations, even though each point in that trajectory is reached at different times.

A specific motion primitive is similar to many motion primitives by noting the effect of velocity and turn rate. The spatial locations of a straight trajectory are generated by a primitive with velocity of $\overline{V}_1$ and duration of $\bar{t}_1$ or by a primitive with velocity of $V_1$ and duration of $(\overline{V}_1/V_1)\bar{t}_1$. The spatial trajectory of a turn trajectory is generated by any primitive with a constant turn radius of $V/\omega$ that rotates by the same angle. The relationship is given in Eq. (8) to find similar primitives given a change in velocity from $\overline{V}_1$ to $V_1$

$$X\left(\bar{t}_1,\overline{V}_1,\overline{\omega}_1,0\right) \sim X\left(\frac{\overline{V}_1}{V_1}\bar{t}_1,V_1,\frac{V_1}{\overline{V}_1}\overline{\omega}_1,0\right) \tag{8}$$

The concept of similarity is applicable to trajectory primitives. A pair of trajectory primitives is similar if they both represent the same spatial locations and attitude orientations despite differences in temporal values. The trajectory primitives of $\overline{T} = \overline{X}_1 + \overline{X}_2 \in \mathcal{T}_2$ and $T = X_1 + X_2 \in \mathcal{T}_2$ are similar if and only if $\overline{X}_1 \sim X_1$ and $\overline{X}_2 \sim X_2$.

A basic relationship for similarity of trajectory primitives is established using Eq. (8). The concept shows the scaling that must occur to maintain the turn radius and distances throughout the trajectories. This relationship is given in Eq. (9)

$$\begin{aligned}&T\left(\bar{t}_1,\bar{t}_2,\overline{V}_1,\overline{V}_2,\overline{\omega}_1,\overline{\omega}_2,0,0\right)\\ &\sim T\left(\frac{\overline{V}_1}{V_1}\bar{t}_1,\frac{\overline{V}_2}{V_2}\bar{t}_2,V_1,V_2,\frac{V_1}{\overline{V}_1}\overline{\omega}_1,\frac{V_2}{\overline{V}_2}\overline{\omega}_2,0,0\right)\end{aligned} \tag{9}$$

## Motion Planning

### Two-Dimensional Optimal Dubins Trajectories

The original formulation of the Dubins car, which is a foundation of the Dubins airplane, has interesting properties for motion planning. This Dubins car operates in a configuration space of $\mathcal{C}^3$ composed of two positions and a heading angle. A pair of results is known for the Dubins car when considering trajectories through an environment without obstacles.

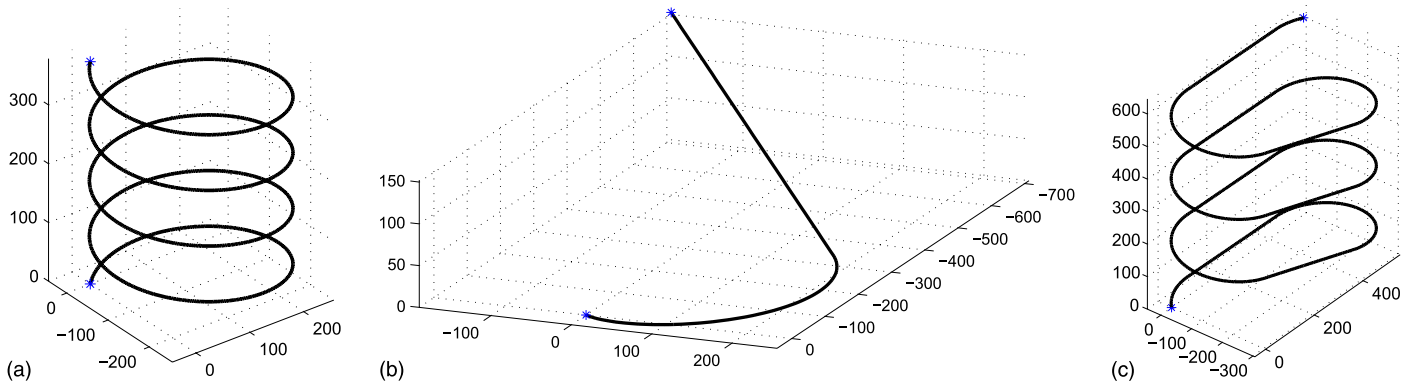


**Fig. 1.** Example of trajectories that start with trajectory primitives that are elements of (a) $\mathcal{T}_1$, (b) $\mathcal{T}_2$, and (c) $\mathcal{T}_3$



J. Aerosp. Eng. 2013.26:571-585.

1. Any position in $\mathcal{R}^2$ can be reached using a two-primitive sequence from any initial configuration in $\mathcal{C}^3$. These sequences are composed of a turn maneuver followed by a straight motion given as either a left-straight sequence or a right-straight sequence. A two-primitive sequence is only able to connect any configuration with any position but cannot guarantee a desired value for the final heading. This optimal trajectory that connects two configurations is computed using the closed-form algebraic expression, as given in Definition 1 (Dubins 1957).
   - Definition 1: Define $\pi_2(C_f - C_o, V, \omega)$ as the closed-form algebraic expression for the trajectory primitive that minimizes time to travel from $C_o \in \mathcal{C}^3$ to $C_f \in \mathcal{R}^2$ using velocity $V$ and turn rate $\omega$. The resulting trajectory primitive, $D_2(t_1, t_2, V, \omega) \in \mathcal{T}_2$, is given as $D_2(t_1, t_2, V, \omega) = \pi_2(C_f - C_o, V, \omega)$.
2. Any configuration in $\mathcal{C}^3$ can be reached using a three-primitive sequence from any initial configuration in $\mathcal{C}^3$. This optimal trajectory is composed of either turn-straight-turn sequences or turn-turn-turn sequences involving a specific sequence of turns being right or left. The resulting trajectory primitive that minimizes time to travel is given in Definition 2 (Dubins 1957).
   - Definition 2: Define $\pi_3(C_f - C_o, V, \omega)$ as the closed-form algebraic expression for the trajectory primitive that minimizes time to travel from $C_o \in \mathcal{C}^3$ to $C_f \in \mathcal{C}^3$ using velocity $V$ and turn rate $\omega$. The resulting trajectory primitive, $D_3(t_1, t_2, t_3, V, \omega) \in \mathcal{T}_3$, is given as $D_3(t_1, t_2, t_3, V, \omega) = \pi_3(C_f - C_o, V, \omega)$.

### Three-Dimensional Optimal Dubins Trajectories

An optimal trajectory is computed that extends the optimal 2D Dubins trajectories. Essentially, the vehicle follows the same path of the optimal 2D trajectory primitive, but an additional vertical motion is introduced from a nonzero climb rate. The concept of similarity is thus critical to demonstrate that the optimal 2D path matches the projection of the optimal 3D path onto the 2D plane.

A pair of results is demonstrated for different requirements on the final configuration. In each case, the vehicle is operating in the configuration space of $\mathcal{C}^4$ composed of three positions and a heading angle.

1. A set of positions in $\mathcal{R}^3$ can be reached using a two-primitive sequence from any initial configuration in $\mathcal{C}^4$. These sequences are composed of a turn maneuver followed by a straight motion given as either a left-straight sequence or a right-straight sequence. This optimal trajectory is given in Definition 3.
   - Definition 3: Define $T_2(t_1, t_2, V_o, V_o, \omega_o, \omega_o, \gamma_1, \gamma_2) \in \mathcal{T}_2$, if it exists, as the optimal trajectory primitive that minimizes travel time from $C_o \in \mathcal{C}^4$ to $C_f \in \mathcal{R}^3$. This primitive satisfies the similarity condition of $T_2(t_1, t_2, V_o, V_o, \omega_o, \omega_o, 0, 0) \sim D_2(t_1, t_2, V_o, \omega_o)$, where $D_2(t_1, t_2, V_o, \omega_o)$ is computed from the closed-form algebraic expression in Definition 1 to connect the projections of $C_o$ onto $\mathcal{C}^3$ to the projection of $C_f$ onto $\mathcal{R}^2$.
2. A set of configurations in $\mathcal{C}^4$ can be reached using a three-primitive sequence from any initial configuration in $\mathcal{C}^4$. This optimal trajectory is composed of either turn-straight-turn sequences or turn-turn-turn sequences involving a specific sequence of turns being right or left. The resulting trajectory primitive that minimizes time to travel is given in Definition 4.
   - Definition 4: Define $T_3(t_1, t_2, t_3, V_o, V_o, V_o, \omega_o, \omega_o, \omega_o, \gamma_1, \gamma_2, \gamma_3) \in \mathcal{T}_3$, if it exists, as the optimal trajectory primitive that minimizes travel time from $C_o \in \mathcal{C}^4$ to $C_f \in \mathcal{C}^4$. This primitive satisfies the similarity condition of $T_3(t_1, t_2, t_3, V_o, V_o, V_o, \omega_o, \omega_o, \omega_o, 0, 0, 0) \sim D_3(t_1, t_2, t_3, V_o, \omega_o)$, where $D_3(t_1, t_2, t_3, V_o, \omega_o)$ is computed from the closed-form algebraic expression in Definition 2 to connect the projections of $C_o$ and $C_f$ onto $\mathcal{C}^3$.

The existence conditions place a limit on altitude; specifically, Definition 3 requires $C_{f_z} - C_{o_z} \leq \gamma_1 t_1 + \gamma_2 t_2$, and Definition 4 requires $C_{f_z} - C_{o_z} \leq \gamma_1 t_1 + \gamma_2 t_2 + \gamma_3 t_3$. These conditions are fundamentally ensuring that the vehicle can move to the required altitude before it reaches the final North-East position.

Also, this formulation requires that all motion primitives, and thus the corresponding trajectory primitives, have uniform values for velocity and turn rate. Such a limitation is required for the algebraic solution from Definition 2; however, this limitation also has the effect of decoupling the climb rate from the velocity and turn rate.

### Three-Dimensional Suboptimal Trajectories

A generalized approach is formulated for motion planning between any pair of configurations. This formulation results in a suboptimal solution for the path; however, this loss of optimality is countered by an increase in solution existence, because a pair of trajectory primitives allows for dramatically more variation than a single trajectory primitive. Also, realistic variations in velocity are allowed by this formulation, and therefore velocity while climbing can be different than velocity while maintaining altitude.

The suboptimal trajectory is determined using a pair of trajectory primitives and an intermediary waypoint. Essentially, a waypoint is determined that separates the operating space and associated motion planning into a pair of trajectories. This grouping of motion primitives into trajectory primitives simplifies the planning and enables the closed-form algebraic expressions of $\pi_2$ and $\pi_3$ to be directly utilized. The resulting paths are thus completely parametrized by the waypoint.

The motion planning uses low-dimension planning to generate a 3D trajectory. Because of the dynamical constraints of the trajectory primitives, the waypoint location fixed along a circle helix can be represented by one parameter, the waypoint location along a turn-straight primitive can be represented as a 2D projection into North-East coordinates (and thus represented by two parameters), and the waypoint location along an oval helix can be represented by three parameters. These parameters (waypoint locations) and the type of trajectory primitive will uniquely determine the trajectory primitive that connects an initial point to the waypoint. This waypoint is chosen to minimize the duration of the optimal 2D trajectory, which is known from the closed-form Dubins solution, from its North-East projection to the North-East projection of the final configuration. The final path has 3D motion through inclusion of a climb rate and constraint of similarity.

The motion planning uses 2D planning to generate a 3D trajectory. The 2D projection into the North-East coordinates of each configuration is used to locate the 2D coordinates of a waypoint. This waypoint is chosen such that the duration of the optimal 2D trajectories, which are known from the closed-form Dubins solutions, has minimal durations in connecting the initial configuration to the waypoint and the waypoint to the final configuration. Another set of trajectories is then identified to follow the same 2D path, using a requirement of similarity, but having 3D motion through inclusion of a climb rate.

This method is extremely efficient for motion planning. The path is a complex trajectory in $\mathcal{C}^4$; however, the search space ranges from $\mathcal{R}^1$ to merely $\mathcal{R}^3$ depending on the type of trajectory primitive. The resulting trajectory primitives are computed from a closed-form algebraic solution and a basic scaling to maintain similarity. As such,



J. Aerosp. Eng. 2013.26:571-585.

a strong utilization of parametric solutions results in solutions, which are suboptimal, but require minor computations to generate.

### *Initial Trajectory Constrained to the Circle Helix*

The specific formulation for motion planning using a circle helix is presented in Eq. (10). The waypoint is restricted to lying along the circumference of the circle associated with the turn radius and the altitude associated with the climb rate; consequently, the location of the waypoint can be determined by a single parameter of $C_w \in \mathcal{R}$. The motion is thus decomposed into a circle helix from the origin to the waypoint followed by the optimal three-sequence primitive, which is determined by a closed-form algebraic solution to the final configuration

$$\min_{C_w \in \mathcal{R}} (t_1 + t_2 + t_3 + t_4) \tag{10}$$

such that

$$T_1(t_1, V_1, \omega_1, \gamma_1) = C_w - C_o \tag{11}$$

$$D_3(\tau_3, \tau_4, \tau_5, V_o, \omega_o) = \pi_3(C_f - C_w, V_o, \omega_o) \tag{12}$$

$$D_3(\tau_2, \tau_3, \tau_4, V_o, \omega_o) \sim T_3(t_2, t_3, t_4, V_2, V_3, V_4, \omega_2, \omega_3, \omega_4, 0, 0, 0) \tag{13}$$

$$C_{f_z} - C_{o_z} \leq \gamma_1 t_1 + \gamma_2 t_2 + \gamma_3 t_3 + \gamma_4 t_4 \tag{14}$$

The cost function in Eq. (10) is determined by the duration of a one-primitive sequence and a three-primitive sequence. The one-primitive sequence, $T_1 \in \mathcal{T}_1$, is directly computed as the unique motion from the initial configuration to the location on the circle defined by $C_w \in \mathcal{R}$, as given in Eq. (11). The final configuration is reached by computing a 2D closed-form algebraic solution in Eq. (12) and then extending into 3D space using a similarity transformation in Eq. (13). The resulting motion must reach the desired altitude, as ensured by the constraint in Eq. (14).

**Table 1.** Aircraft Parameters

| Primitive | Velocity (m/s) | Climb rate (m/s) | Turn rate (rad/s) |
|---|---|---|---|
| Straight, level | 40 | 0 | 0 |
| Turn, level | 30 | 0 | 0.2 |
| Straight, climb | 25 | 4 | 0 |
| Turn, climb | 20 | 2 | 0.13 |
| Straight, dive | 50 | −6 | 0 |
| Turn, dive | 35 | −4 | 0.23 |

**Table 2.** Final Configurations

| Configuration | North (m) | East (m) | Altitude (m) | Heading (degrees) |
|---|---|---|---|---|
| $C_{f_1}$ | 600 | −150 | 300 | 0 |
| $C_{f_2}$ | 600 | −450 | 375 | 12 |
| $C_{f_3}$ | 600 | −450 | 900 | 12 |

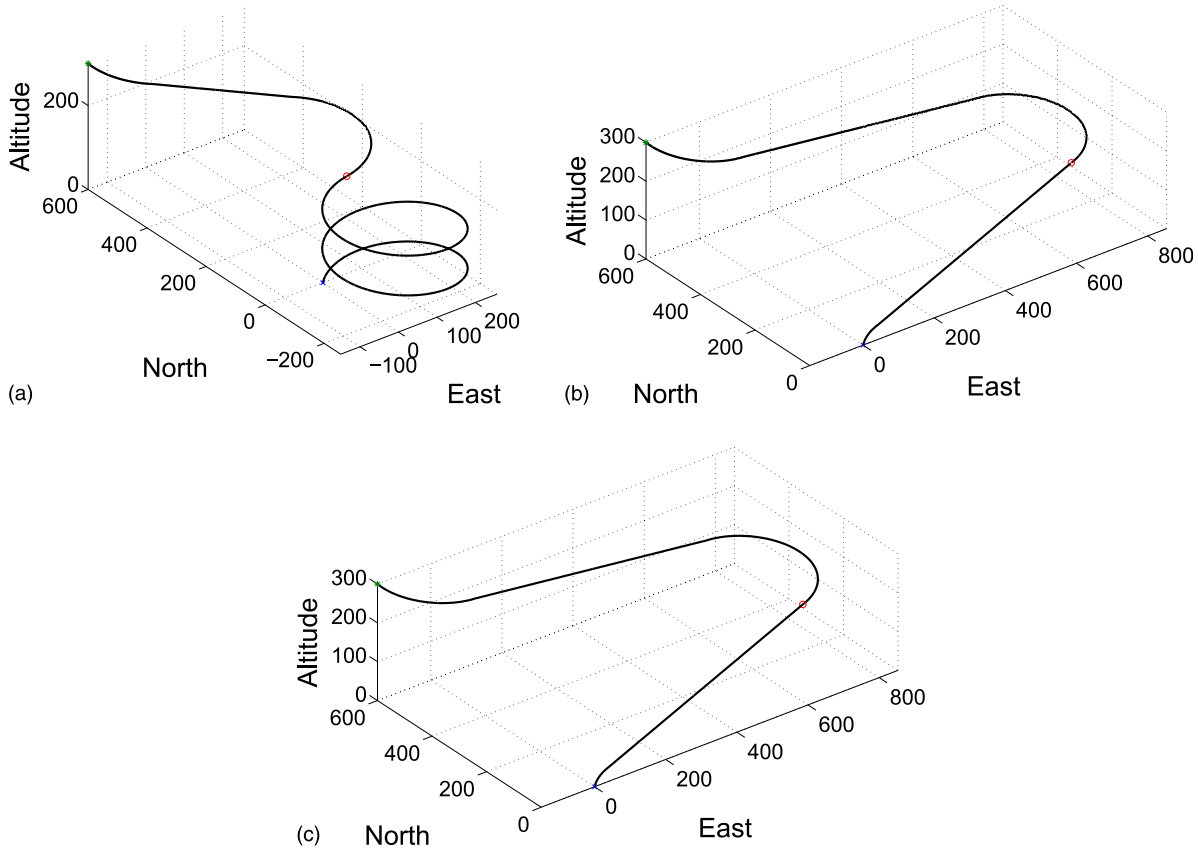


**Fig. 2.** (a) Trajectory from $C_o$ to $C_{f_1}$ using one-primitive circle, (b) two-primitive monotonic, and (c) four-primitive oval



J. Aerosp. Eng. 2013.26:571-585.

### Initial Trajectory Constrained to Monotonic Motion

The formal statement for motion planning that requires monotonic motion, which implies that revolutions are not allowed, is minimizing the cost function given in Eq. (15). The planning merely searches over the waypoint coordinates, $C_w \in \mathcal{R}^2$, for the optimization. In this case, each trajectory primitive that connects with the waypoint is computed from the closed-form algebraic solutions in a 2D plane and simply extended into 3D paths by introducing a climb rate through a similarity constraint (Pachikara et al. 2009)

$$\min_{C_w \in \mathcal{R}^2} (t_1 + t_2 + t_3 + t_4 + t_5) \tag{15}$$

such that

$$D_2(\tau_1, \tau_2, V_o, \omega_o) = \pi_2(C_w - C_o, V_o, \omega_o) \tag{16}$$

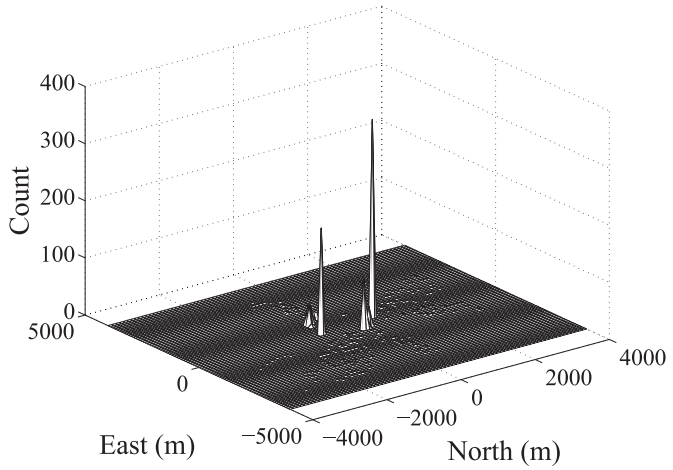


**Fig. 3.** Histogram of the waypoint position from $C_o$ to $C_{f_1}$ using a two-primitive trajectory

$$D_3(\tau_3, \tau_4, \tau_5, V_o, \omega_o) = \pi_3(C_f - C_w, V_o, \omega_o) \tag{17}$$

$$D_2(\tau_1, \tau_2, V_o, \omega_o) \sim T_2(t_1, t_2, V_1, V_2, \omega_1, \omega_2, 0, 0) \tag{18}$$

$$D_3(\tau_3, \tau_4, \tau_5, V_o, \omega_o) \sim T_3(t_3, t_4, t_5, V_3, V_4, V_5, \omega_3, \omega_4, \omega_5, 0, 0, 0) \tag{19}$$

$$C_{f_z} - C_{o_z} \leq \gamma_1 t_1 + \gamma_2 t_2 + \gamma_3 t_3 + \gamma_4 t_4 + \gamma_5 t_5 \tag{20}$$

The cost function in Eq. (15) is determined by the duration of the trajectory primitives, $T_2 \in \mathcal{T}_2$ and $T_3 \in \mathcal{T}_3$, that connect $C_o$ to $C_f$. The process generates the optimal 2D Dubins solutions using the closed-form algebraic solutions, as noted in the constraints of Eqs. (16) and (17). These 2D paths are extended into 3D environments by the similarity constraints in Eqs. (18) and (19) by introducing a climb rate and scaling for variations in velocity and the climb rate. Finally, the constraint on altitude is enforced through Eq. (20) to ensure the vehicle has sufficient time to climb or dive.

### Initial Trajectory Constrained to the Oval Helix

The formulation given in Eq. (21) relates the cost associated with computing motion using a four-primitive oval helix. The initial primitive based on that oval is parametrized around three variables, whereas the final primitive is again the unique closed-form solution based on Dubins' path; consequently, the optimization searches over a 3D design space, which is expressed as the coordinates of the waypoint

$$\min_{C_w \in \mathcal{R}^3} (t_1 + t_2 + t_3 + t_4 + t_5 + t_6) \tag{21}$$

such that

$$T_4(t_1, t_2, t_3, V_1, V_2, \omega_1, \omega_2, \gamma_1, \gamma_2) = C_w - C_o \tag{22}$$

$$D_3(\tau_4, \tau_5, \tau_6, V_o, \omega_o) = \pi_3(C_f - C_w, V_o, \omega_o) \tag{23}$$

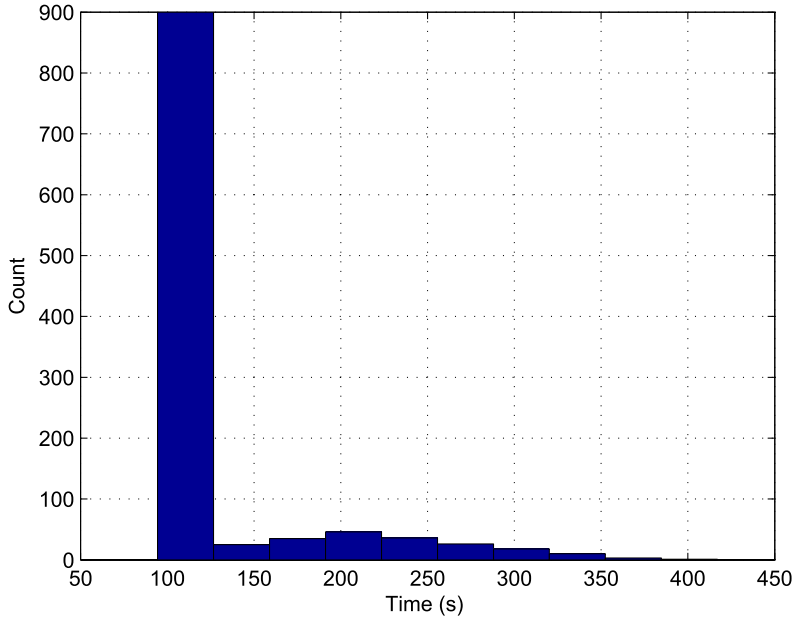


**Fig. 4.** Histogram of the trajectory duration from $C_o$ to $C_{f_1}$ using a two-primitive trajectory



J. Aerosp. Eng. 2013.26:571-585.

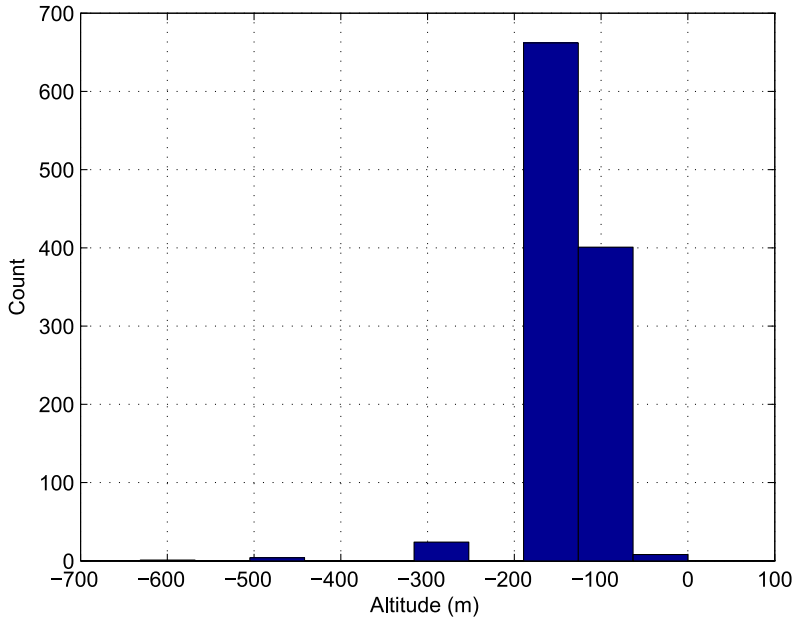


**Fig. 5.** Histogram of the waypoint altitude from $C_o$ to $C_{f_1}$ using a four-primitive trajectory

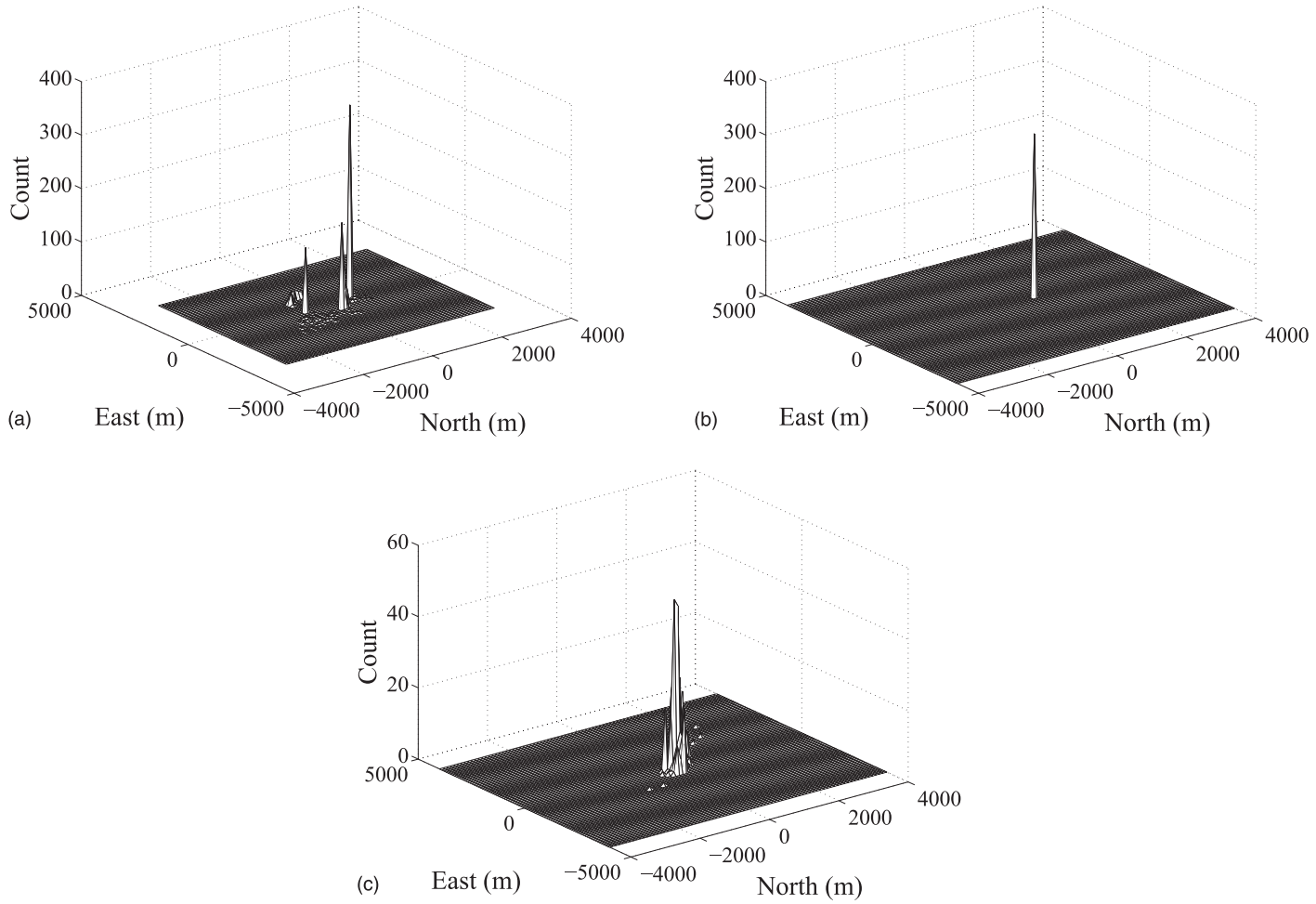


**Fig. 6.** (a) Histogram of the waypoint coordinates in the East and North from $C_o$ to $C_{f_1}$ for an altitude of −143.41 m, (b) −119.43 m, and (c) outliers



J. Aerosp. Eng. 2013.26:571-585.

$$D_3(\tau_4, \tau_5, \tau_6, V_o, \omega_o) \sim T_3(t_4, t_5, t_6, V_4, V_5, V_6, \omega_4, \omega_5, \omega_6, 0, 0, 0) \tag{24}$$

$$C_{f_z} - C_{o_z} \leq \gamma_1 t_1 + \gamma_2 t_2 + \gamma_3 t_3 + \gamma_4 t_4 + \gamma_5 t_5 + \gamma_6 t_6 \tag{25}$$

The cost function for this planning in Eq. (21) results from the durations of the pair of trajectory primitives. The initial primitive is the oval that connects the initial configuration to a waypoint, as given in Eq. (22). That waypoint is used to generate an optimal 2D primitive in Eq. (23) and then a suboptimal 3D primitive using a similarity relationship in Eq. (24). The final constraint in Eq. (25) ensures the entire motion has sufficient change in altitude.

## Example

### Motion Primitives

A set of motion primitives is generated in Table 1 to represent feasible maneuvers for a class of small aircraft. The velocity varies between each primitive to note a faster airspeed during dives and slower airspeed during climbs. The variations in turn rates are chosen such that a constant value of 150 m is maintained for the turn radius.

### Trajectories without Airspace Constraints

Motion planning is performed for the aircraft to travel from an initial condition of $C_o = (0, 0, 0, 45°)$ to a set of final conditions. These final conditions, as given in Table 2, have varied position and altitude.

A Monte Carlo analysis is performed on the motion planning to evaluate the variations in resulting trajectories. In this case, 1,100 different values of the initial condition for the waypoint are randomly selected. The ensuing optimization searches over a nonlinear function, and therefore the initial condition has an effect on the local minimum associated with the resulting trajectory. The use of the one-primitive circle results in a one-dimensional optimization for which a single waypoint was identified each time, and therefore associated statistics are not presented.

The computation times are not presented in each case, because the times are always on the order of a few seconds. Each optimization simply uses the fmincon command in *MATLAB* while running on a desktop computer.

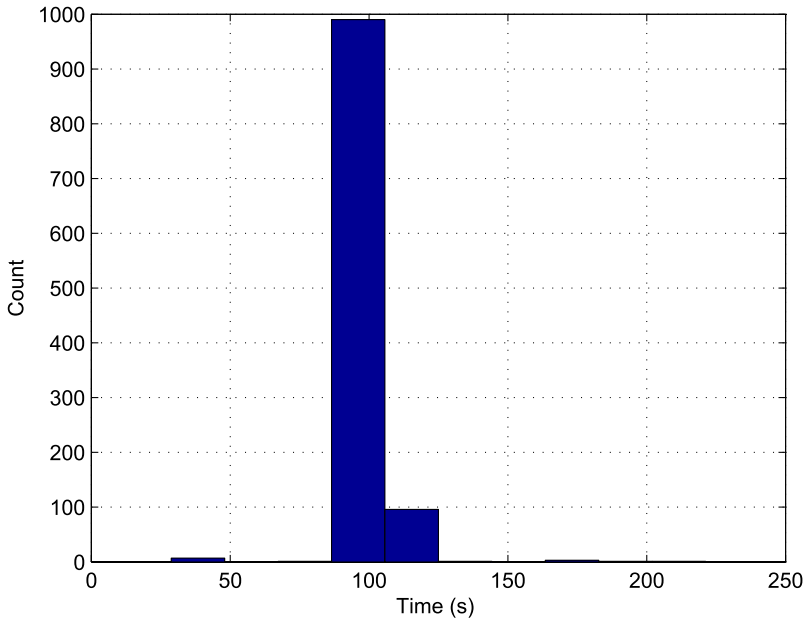


**Fig. 7.** Histogram of the trajectory duration from $C_o$ to $C_{f_1}$ using a four-primitive trajectory

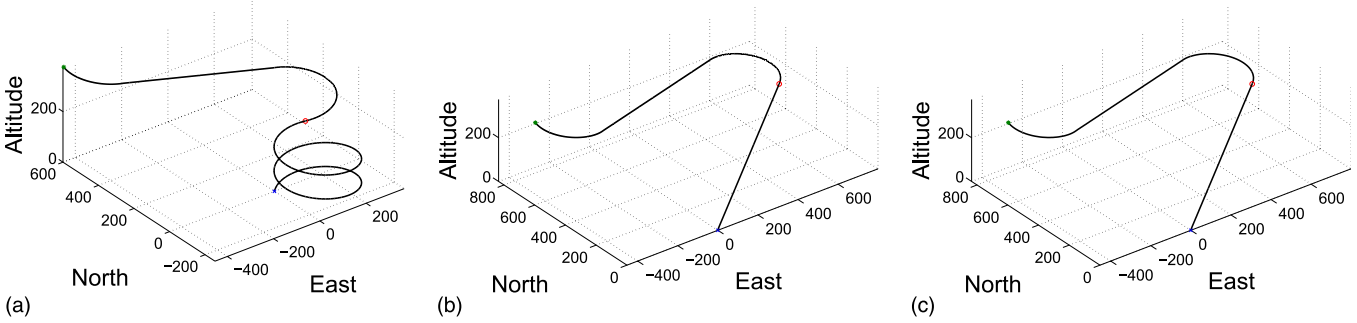


**Fig. 8.** (a) Trajectory from $C_o$ to $C_{f_2}$ using 1-primitive circle, (b) two-primitive monotonic, and (c) four-primitive oval



J. Aerosp. Eng. 2013.26:571-585.

### Motion Planning from $C_o$ to $C_{f_1}$

A set of trajectories is computed using the various forms of trajectory primitives to connect $C_o$ with $C_{f_1}$, as shown in Fig. 2. The use of one-primitive circles results in a total time of 138 s, and the use of either the two-primitive trajectory or four-primitive oval results in a total time of 95 s. In this case, the similarity for the two-primitive trajectory and four-primitive oval is a direct result of the low climb rate associated with turning. The optimization seeks to maximize the length of any straight segments and minimize the amount of turns; consequently, the optimal oval is simply a half-oval shape with a single turn, which thus matches the straight-turn combination associated with a two-primitive trajectory.

The optimization for motion planning using the two-primitive monotonic motion searches over a 2D space East and North for the waypoint. Most waypoints identified by the optimization, despite variations in an initial condition for that waypoint, are located at a few distinct locations, as shown in Fig. 3. Such a result indicates that only a limited number of waypoints can be connected by optimal trajectories and still reach the desired altitude.

The histogram in Fig. 4 shows the values of trajectory duration for each waypoint in Fig. 3. These values indicate that several waypoints are local minima for the optimization; however, they result in nearly the same cost. The minimum duration is 94.44 s, and the maximum duration is 416.96 s with a mean of 121.31 s and an SD of 55.12 s. Still, the optimization mostly found values near the minimum.

The optimization using the four-primitive ovals requires searching over a 3D space. As such, the resulting waypoint must be noted for both the East and the North along with altitude. The histogram of that altitude is given in Fig. 5 and indicates that two altitudes, −143.41 and −119.43 m, are primarily found by the optimization.

The coordinates of the East and the North for the resulting waypoints are shown in Fig. 6. These results indicate that the optimization found only a pair of waypoints in most cases, because unique values of the East and the North are found at each altitude. In this case, the altitude of −143.41 m, which appeared in 160 of the trajectories, is associated with coordinates of 1,192.02 and 1,294.69 m, whereas the altitude of −119.43 m, which appeared in 306 of the trajectories, is associated with coordinates of 200.08 and 742.98 m. Even the waypoints that are outliers in terms of altitude still have coordinates for the East and the North that are similar to the primary waypoints.

The duration of the motion associated with the various waypoints and associated trajectory primitives is shown in Fig. 7. These durations are nearly identical in most of the cases implying that the pair of waypoints is local minima with similar costs.

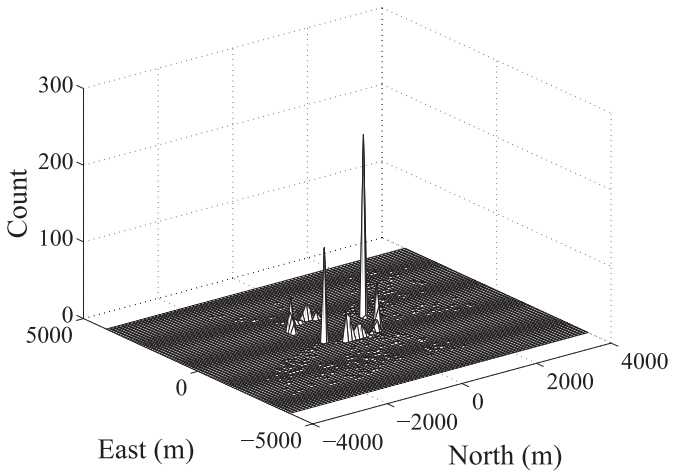


**Fig. 9.** Histogram of the waypoint position from $C_o$ to $C_{f_2}$ using a two-primitive trajectory

### Motion Planning from $C_o$ to $C_{f_2}$

The motion planning generates trajectories from $C_o$ to $C_{f_2}$, as shown in Fig. 8. The one-primitive circle requires a total time of 164 s, whereas the two-primitive monotonic and four-primitive oval require 113 s. Again, the cost associated with turning is evident in the circle motion and the convergence of the oval motion to the monotonic motion.

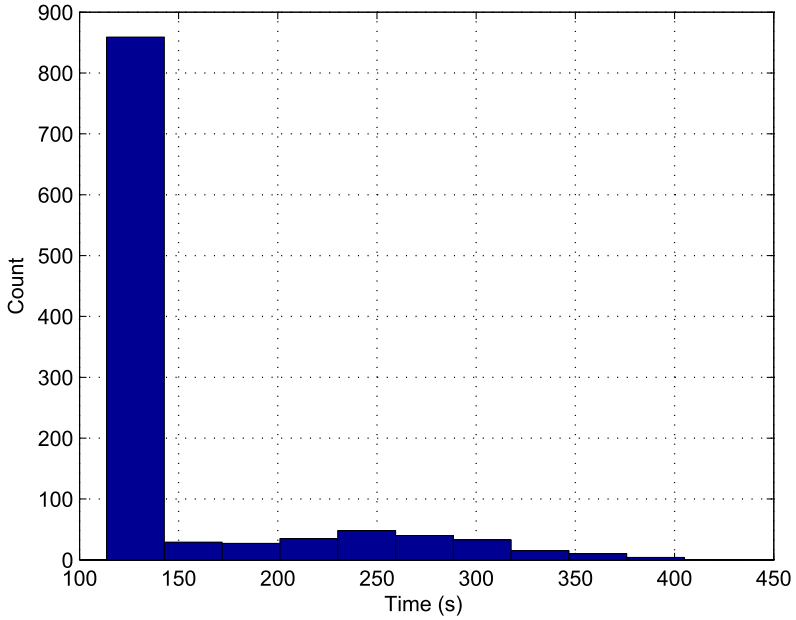


**Fig. 10.** Histogram of the trajectory duration from $C_o$ to $C_{f_2}$ using a two-primitive trajectory



J. Aerosp. Eng. 2013.26:571-585.

The waypoints associated with the two-primitive monotonic motions are shown in Fig. 9. The locations of these waypoints are scattered somewhat throughout the design space with small peaks at several locations.

The histogram in Fig. 10 shows the values of trajectory duration for each waypoint in Fig. 9. Most trajectories, despite the variation in waypoint location, have the same duration. The entire set has a range from 113.66 to 405.06 s, but most trajectories are computed with durations near the minimum.

The statistics of the optimization using the four-primitive ovals is also generated using a Monte Carlo analysis. In this case, the altitudes associated with the waypoint for this 3D design space are shown in Fig. 11. A single altitude of −149.69 m is clearly dominant in the data.

The coordinates of the East and the North for the resulting waypoints are shown in Fig. 12. A single waypoint with coordinates of 565.45 and 739.80 m is uniquely associated with the altitude of −149.69 m. The waypoints associated with the outliers in altitudes differ somewhat but remain centered around these same coordinates.

The duration of the motion associated with the various waypoints and associated trajectory primitives is shown in Fig. 13. These durations are nearly identical in most of the cases to imply that the optimization found a single cost almost uniformly.

### Motion Planning from $C_o$ to $C_{f_3}$

The final trajectories, shown in Fig. 14, connect $C_o$ to the high-altitude configuration of $C_{f_3}$. These paths require 433 s using a circle motion but only 246 s using the monotonic motion or an oval motion. Clearly the cost associated with turning creates a noticeable disadvantage to the planning that uses circles to achieve altitude.

The waypoints associated with the two-primitive monotonic motions are shown in Fig. 15. The locations of these waypoints show a clear pattern of lying in a circle. A peak occurs at one value; however, a reasonable number of waypoints is varied along the circle.

The histogram in Fig. 16 shows the values of trajectory duration for each waypoint in Fig. 15. The trajectories range from 245.94 to 418.38 s; however, they have predominately the same duration. As

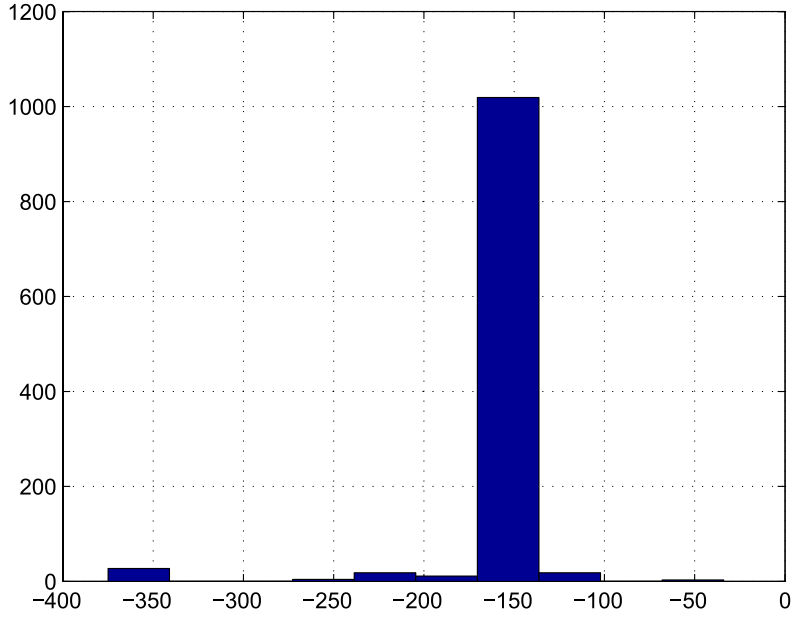


**Fig. 11.** Histogram of the waypoint altitude from $C_o$ to $C_{f_2}$ using a four-primitive trajectory

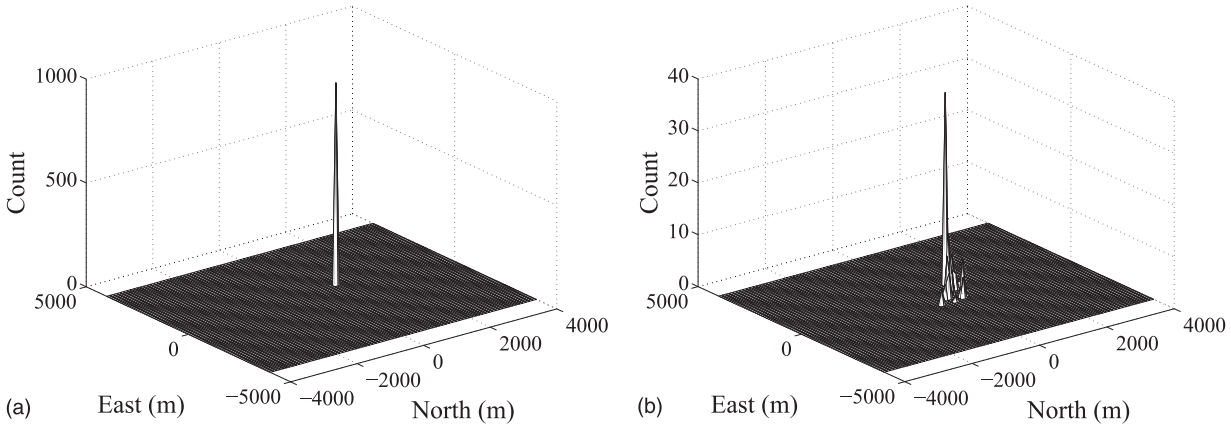


**Fig. 12.** (a) Histogram of the waypoint coordinates in the East and North from $C_o$ to $C_{f_2}$ for an altitude of −149.69 m and (b) outliers

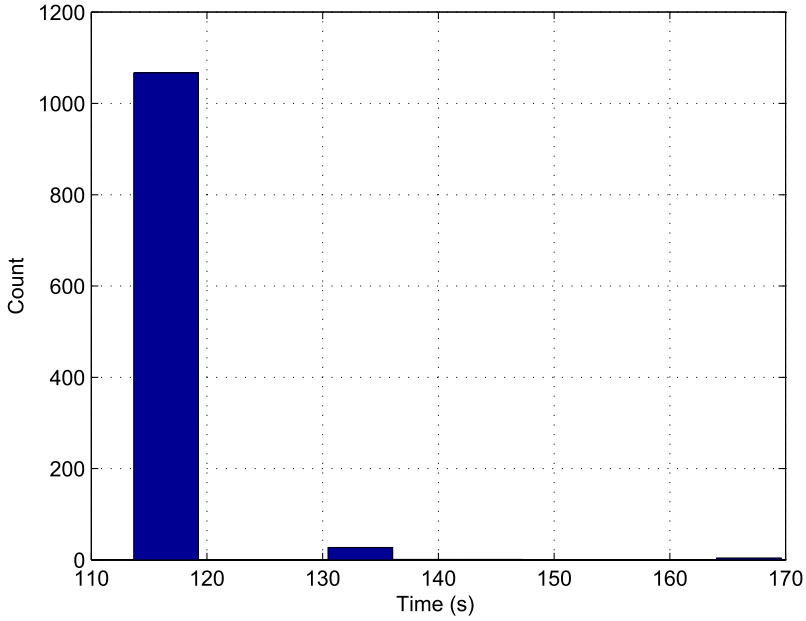


**Fig. 13.** Histogram of the trajectory duration from $C_o$ to $C_{f_2}$ using a four-primitive trajectory

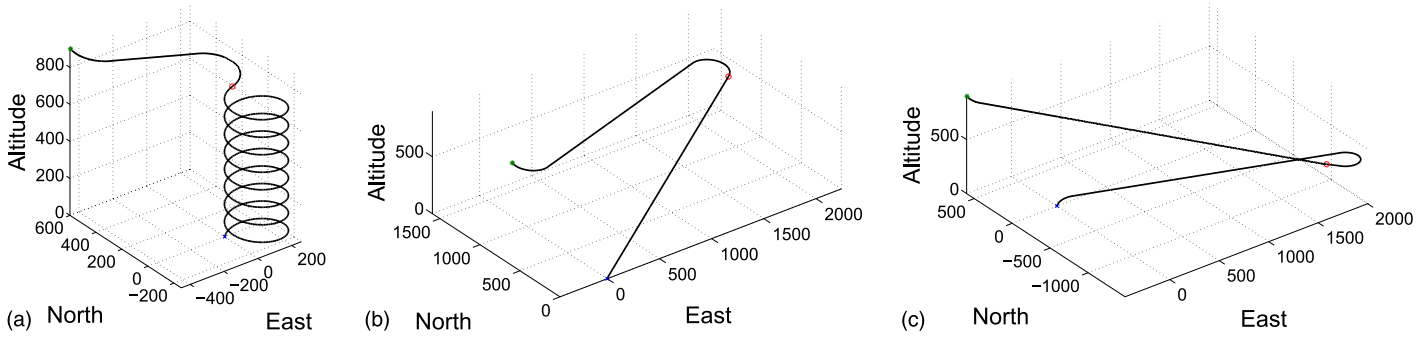


**Fig. 14.** (a) Trajectory from $C_o$ to $C_{f_3}$ using one-primitive circle, (b) two-primitive monotonic, and (c) four-primitive oval

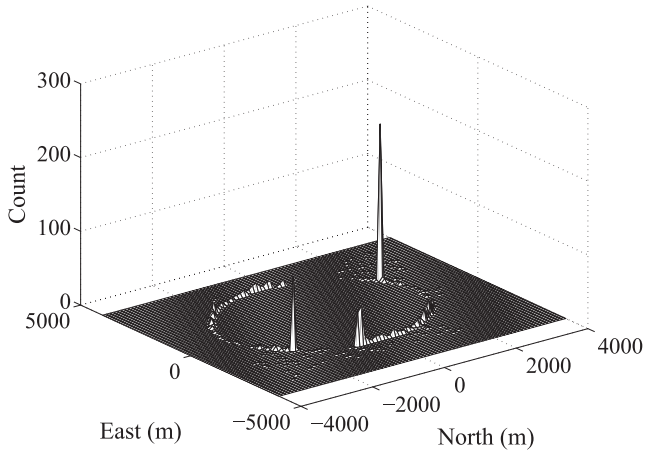


**Fig. 15.** Histogram of the waypoint position from $C_o$ to $C_{f_3}$ using a two-primitive trajectory

such, the circle of locations in Fig. 15 is a set of local minima associated with the same duration of motion.

The use of four-primitive ovals introduces the additional parameter of altitude to the design space of the East and the North. These altitudes for the connection of $C_o$ to $C_{f_3}$ are shown in the histogram of Fig. 17. Most waypoints are found at an altitude of $-411.17$ m with another set at $-900.00$ m and some remaining scattered across intervening altitudes.

The coordinates of the East and the North for the resulting waypoints are shown in Fig. 18. These results indicate that the optimization found only a pair of waypoints in most cases, because unique values of the East and the North are found at each altitude. In this case, the altitude of $-900.00$ m, which appeared in 234 of the trajectories, is associated with coordinates of 307.81 and 741.20 m, whereas the altitude of $-411.17$ m, which appeared in 660 of the trajectories, is associated with coordinates of 1,405.13 and 2,125.58 m. Even the waypoints that are outliers in terms of altitude still have coordinates for the East and the North, which are similar to the primary waypoints.

The duration of the motion associated with the various waypoints and trajectory primitives is shown in Fig. 19. In this case, the trajectories using a waypoint with an altitude of $-900.00$ m have a



J. Aerosp. Eng. 2013.26:571-585.

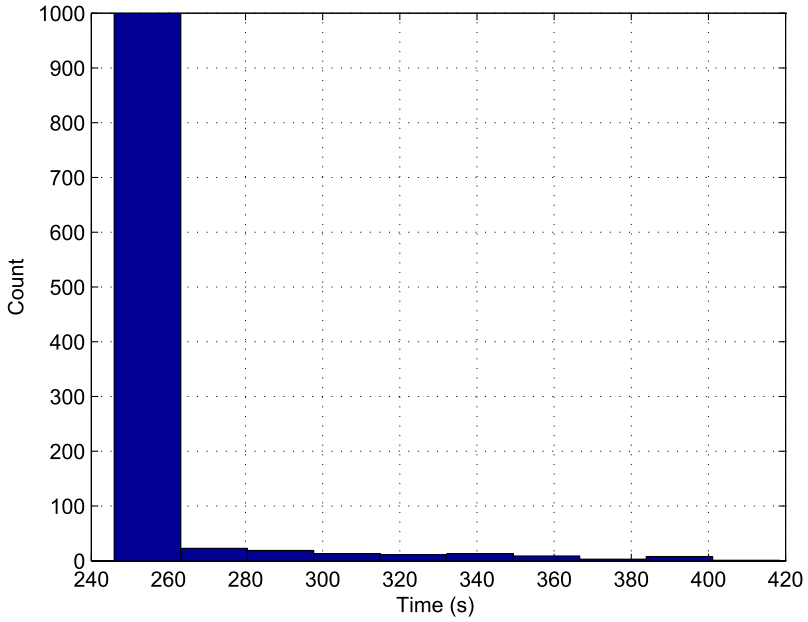


**Fig. 16.** Histogram of the trajectory duration from $C_o$ to $C_{f_3}$ using a two-primitive trajectory

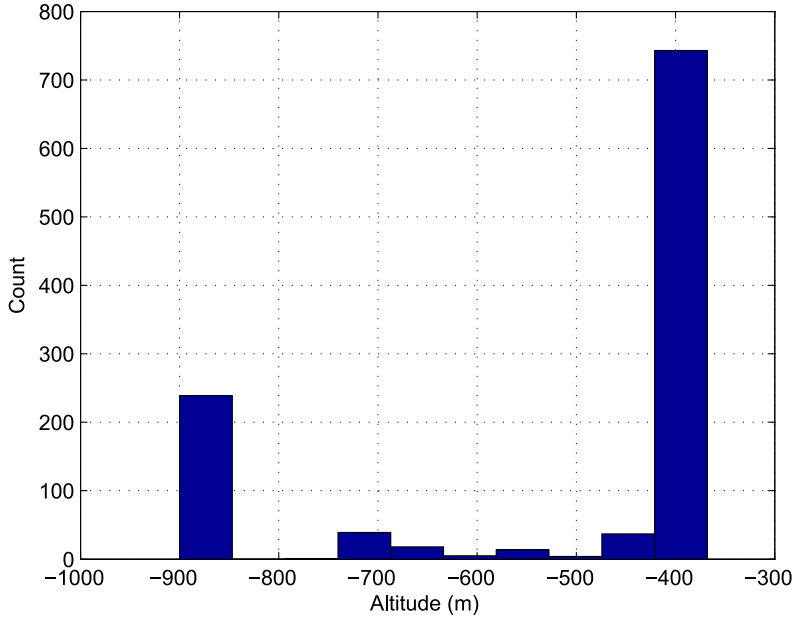


**Fig. 17.** Histogram of the waypoint altitude from $C_o$ to $C_{f_3}$ using a four-primitive trajectory

unique duration, whereas those with any other altitude had a slightly longer duration.

### *Trajectories with Airspace Constraints*

A scenario involving airspace constraints is also simulated. In this case, the initial location of the aircraft lies within a box ranging from −600 to 800 m along the East and −400 to 800 m along the North. The vehicle must travel from $C_o$ to $C_{f_3}$ while remaining within this box.

The resulting motions are given in Fig. 20 for each of the trajectory primitives. The one-primitive circle takes a duration of 432.90 s and the four-primitive oval requires 293.87 s, whereas the two-primitive monotonic takes only 245.94 s. The motion using a two-primitive monotonic minimizes turns and the associated penalty in climb rate; however, that motion also violates the airspace constraints. As such, the introduction of the four-primitive ovals allows an optimal trajectory that can balance motion characteristics and airspace constraints.

## Conclusions

This paper demonstrates a method of path parametrization to enable motion planning of 3D trajectories. The method introduces a waypoint that divides the resulting trajectory into a pair of smaller

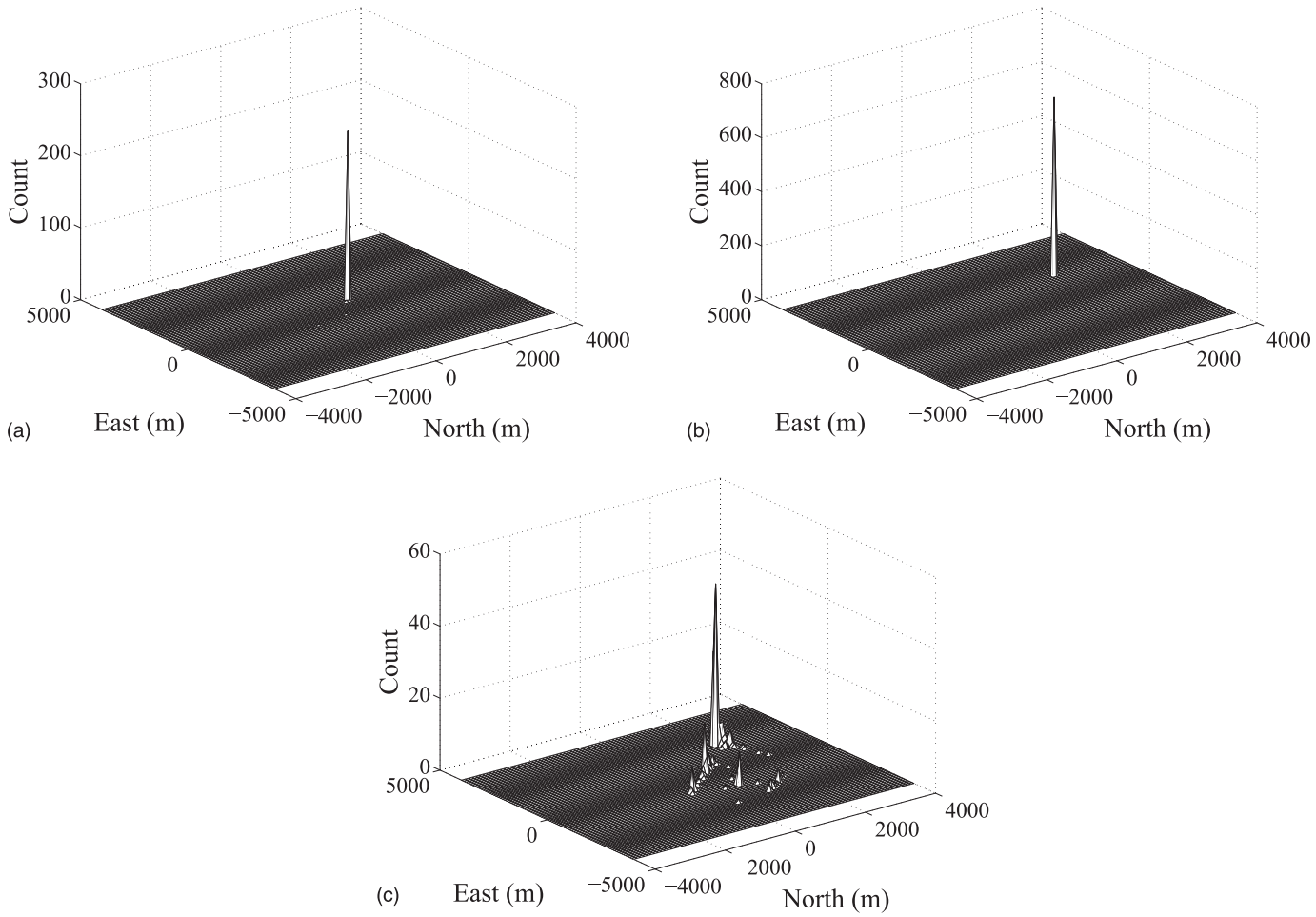


**Fig. 18.** (a) Histogram of the waypoint coordinates in the East and North from $C_o$ to $C_{f_3}$ for an altitude of −900.00 m, (b) −411.17 m, and (c) outliers

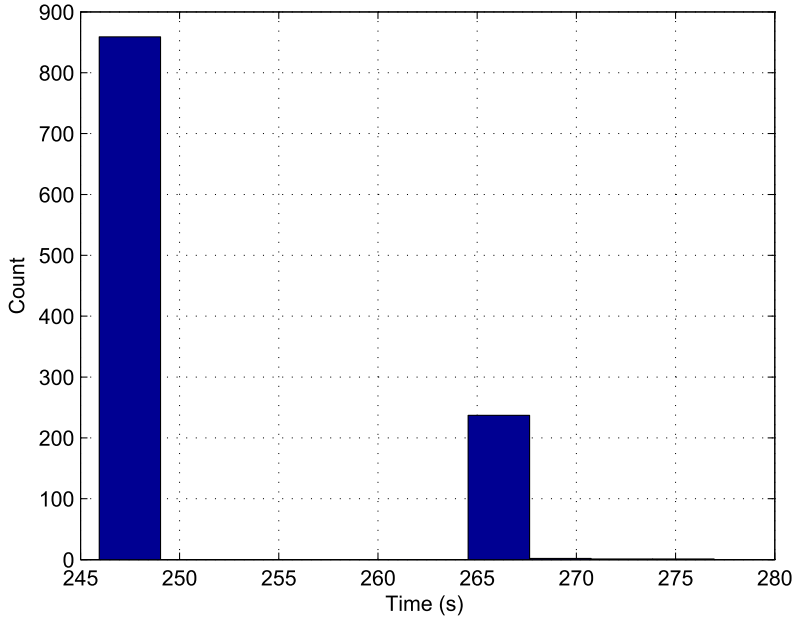


**Fig. 19.** Histogram of the trajectory duration from $C_o$ to $C_{f_3}$ using a four-primitive trajectory



J. Aerosp. Eng. 2013.26:571-585.

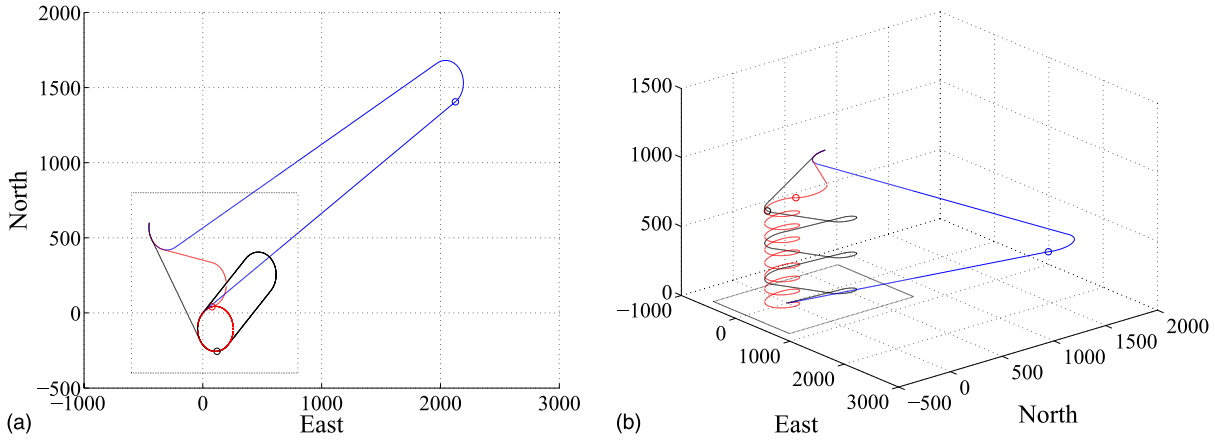


**Fig. 20.** (a) Motions from $C_o$ to $C_{f_3}$ using one-primitive circles, two-primitive monotonic, and four-primitive ovals as viewed from above and (b) angle

trajectories. A concept of trajectory primitives, which can be efficiently computed using closed-form algebraic solutions, is used to connect the waypoint to the original and final configuration. These trajectory primitives are described as a circular helix or oval helix, which admit periodic revolutions over a East-North path, or a monotonic motion, which does not admit revolutions. The resulting optimization of a complicated path only requires searching over a low-dimensional space associated with the waypoint coordinates. A set of trajectories is generated for a vehicle simulation to show the ability to reach a desired location and heading at different altitudes with potential airspace constraints. A Monte Carlo analysis is performed by considering the trajectories resulting from 1,100 different initial conditions. The trajectory is generated using a nonlinear optimization, and is therefore not guaranteed to be optimal; however, the statistics indicate any choice of initial condition has roughly a 90% probability of resulting in an optimal trajectory for the example being considered. Such a high probability is not guaranteed for every example but certainly gives some confidence that the lack of guaranteed optimality may be acceptable given the low computational cost of motion planning.

## Notation

*The following symbols are used in this paper:*

$C$ = configuration;
$\mathcal{C}$ = configuration space;
$p$ = position;
$T$ = trajectory primitive;
$\mathcal{T}$ = set of trajectory primitives;
$t$ = time;
$V$ = velocity;
$\mathcal{V}$ = set of velocities;
$X$ = motion primitive;
$\mathcal{X}$ = set of motion primitives;
$\Gamma$ = set of climb rates;
$\gamma$ = climb rate;
$\pi$ = closed-form algebraic expression for a trajectory primitive;
$\tau$ = time;
$\Psi$ = heading angle;
$\Omega$ = set of turn rates; and
$\omega$ = turn rate.

### Subscripts

$x, y, z$ = coordinates of the North, East, and altitude, respectively.

## References


Ambrosino, G., Ariola, M., Ciniglio, U., Corraro, F., and Pironti, A. (2006). "Algorithms for 3D UAV path generation and tracking." *Proc., 45th IEEE Conf. Decision Control*, IEEE, New York, 5275–5280.

Chitsaz, H., and LaValle, S. M. (2007). "On time-optimal paths for the Dubins airplane." *Proc., 46th IEEE Conf. Decision Control*, IEEE, New York, 2379–2384.

Dubins, L. (1957). "On curves of minimal length with a constraint on average curvature and with prescribed initial and terminal positions and tangents." *Am. J. Math.*, 79(3), 497–516.

Grymin, D. J., and Crassidis, A. (2009). "Simplified model development and trajectory determination for a UAV using the Dubins set." *Proc., AIAA Guidance, Navigation, Control Conf.*, AIAA, Reston, VA.

Howlett, J., Goodrich, M., and McLain, T. (2003). "Learning real-time *A** path planner for sensing closely-spaced targets from an aircraft." *Proc., AIAA Guidance, Navigation, Control Conf.*, AIAA, Reston, VA.

Hurley, R., Lind, R., and Kehoe, J. J. (2009). "A mixed local-global solution to motion planning within 3-D environments." *Proc., AIAA Guidance, Navigation, Control Conf.*, AIAA, Reston, VA.

Kuwata, Y., and How, J. (2004). "Three dimensional receding horizon control for UAVs." *Proc., AIAA Guidance, Navigation, Control Conf.*, AIAA, Reston, VA.

Larson, R. A., Pacther, M., and Mears, M. J. (2005). "Path planning by unmanned air vehicles for engaging an integrated radar network," *Proc., AIAA Guidance, Navigation, Control Conf.*, AIAA, Reston, VA.

Le Ny, J., and Feron, E. (2005). "An approximation algorithm for the curvature-constrained traveling salesman problem." *Proc., 43rd Annual Allerton Conf. Comm. Control Comput.*, Curran Associates, Inc., Red Hook, NY, 620–629.

Malaek, S. M., and Nabavi, S. Y. (2010). "Near-optimal trajectories to manage landing sequence in the vicinity of controlled aerodrones." *J. Aircr.*, 47(1), 129–140.

*MATLAB R2012b* [Computer software]. Natick, MA, The Mathworks, Inc.

McGee, T. G., and Hedrick, J. K. (2007). "Optimal path planning with a kinematic airplane model." *J. Guid. Control Dyn.*, 30(2), 629–633.

Pachikara, A. J., Kehoe, J. J., and Lind, R. (2009). "A path-parametrization approach using trajectory primitives for 3-dimensional motion planning." *Proc., AIAA Guidance, Navigation, Control Conf.*, AIAA, Reston, VA.

Scholer, F., La Cour-Harbo, A., and Bisgaard, M. (2009). "Collision free path generation in 3D with turning and pitch radius constraints for

aerial vehicles." *Proc., AIAA Guidance, Navigation, Control Conf.*, AIAA, Reston, VA.
Shanmugavel, M., Tsourdos, A., Zbikowski, R., and White, B. A. (2005). "Path planning of multiple UAVs using Dubins sets." *Proc., AIAA Guidance, Navigation, Control Conf.*, AIAA, Reston, VA.
Shanmugavel, M., Tsourdos, A., Zbikowski, R., and White, B. A. (2006). "3D Dubins sets based coordinated path planning for swarm of UAVs." *Proc., AIAA Guidance, Navigation, Control Conf.*, AIAA, Reston, VA.
Shima, T., Rasmussen, S., and Gross, D. (2007). "Assigning micro UAVs to task tours in an urban terrain." *IEEE Trans. Contr. Syst. Technol.*, 15(4), 601–612.
Shkel, A., and Lumelsky, V. (2001). "'Classification of the Dubins set." *Robot. Auton. Syst.*, 34(4), 179–202.
Sujit, P., and Beard, R. (2007). "Multiple MAV task allocation using distributed auctions." *Proc., AIAA Guidance, Navigation, Control Conf.*, AIAA, Reston, VA.
Tang, Z., and Ozguner, U. (2005). "Motion planning for multitarget surveillance with mobile sensor agents." *IEEE Trans. Robot.*, 21(5), 898–908.
Yang, G., and Kapila, V. (2002). "Optimal path planning for unmanned vehicles with kinematic and tactical constraints." *Proc., 41st IEEE Conf. Decision Control*, IEEE, New York, 1301–1306.
Zollars, M., Blue, P., and Burns, B. (2007). "Wind corrected flight path planning for autonomous micro air vehicles utilizing optimization techniques." *Proc., AIAA Guidance, Navigation, Control Conf.*, AIAA, Reston, VA.





J. Aerosp. Eng. 2013.26:571-585.